Online: https://jurnal.fk.uisu.ac.id/index.php/ibnusina

Ibnu Sina: Jurnal Kedokteran dan Kesehatan-Fakultas Kedokteran Universitas Islam Sumatera Utara

ISSN 1411-9986 (Print) | ISSN 2614-2996 (Online)

Artikel Penelitian

ANALISIS KORELASI SPEKTRUM HISTOMORFOLOGI RADANG GRANULOMATOSA TUBERKULOSIS DENGAN KEPADATAN INFILTRASI ACID-FAST BACILLI

CORRELATION ANALYSIS OF THE HISTOMORPHOLOGICAL SPECTRUM OF TUBERCULOUS GRANULOMATOUS INFLAMMATION WITH ACID-FAST BACILLI DENSITY

Delyuzar[a*], Causa Trisna Mariedina[a], Betty[a], T. Kemala Intan[a], Arie Widiansyah Hasibuan[a]

[a]Department of Anatomical Pathology Universitas Sumatera Utara, Jl. Universitas No.1 Abdul Hakim Building 1st Floor, Medan, 20154, Indonesia

Histori Artikel

Diterima:
4 Februari 2026

Revisi:
18 Februari 2026

Terbit:
1 Juli 2026

Kata Kunci

Tuberkulosis, granuloma, histomorfologi, *Acid-Fast Bacilli*, *Modified Ziehl–Neelsen*

A B S T R A K

Spektrum histomorfologi radang granulomatosa tuberkulosis diperkirakan mencerminkan dinamika replikasi basil dan respons imun. Penelitian ini merupakan studi analitik observasional dengan desain *cross-sectional* yang dilakukan secara retrospektif melalui peninjauan data sekunder rekam medis serta arsip slide histopatologi dan blok parafin, untuk menganalisis korelasi dan kekuatan hubungan antara spektrum histomorfologi radang granulomatosa tuberkulosis pada pewarnaan *Hematoxylin–Eosin* dengan kepadatan *acid-fast bacilli* (AFB) pada pewarnaan *Modified Ziehl–Neelsen*, di Unit Patologi Anatomik Rumah Sakit Pendidikan Prof. dr. Chairuddin Panusunan Lubis USU Medan dan Rumah Sakit Columbia Asia Medan, pada periode 2023–2025 dengan *consecutive sampling*; 68 kasus memenuhi kriteria inklusi. Spektrum histomorfologi diklasifikasikan menjadi granuloma epiteloid dengan atau tanpa sel datia *Langhans* disertai massa nekrosis, granuloma epiteloid dengan atau tanpa sel datia *Langhans* tanpa massa nekrosis dan *acellular eosinophilic mass* dengan sel-sel inflamasi. Kepadatan *AFB* dilaporkan menggunakan sistem klasifikasi semi-kuantitatif (0, +1, +2, +3) pada pembesaran 1000×. Analisis dilakukan menggunakan uji eksak *Fisher-Freeman-Halton* dan *Cramer's V*. Mayoritas kasus ekstrapulmonal (95,59%), tipe granuloma epiteloid dengan nekrosis (69,12%), dan skor AFB +1 (67,65%). Terdapat korelasi bermakna antara spektrum histomorfologi dan kepadatan AFB ($p<0.001$) dengan kekuatan hubungan kuat (*Cramer's V*=0.59). Korelasi spektrum histomorfologi maupun kepadatan AFB terhadap kelompok organ, umur, dan jenis kelamin tidak bermakna ($p>0.05$).

Keywords

Tuberculosis, granuloma, histomorphology, Acid-Fast Bacilli, Modified Ziehl–Neelsen

A B S T R A C T

The histomorphological spectrum of tuberculous granulomatous inflammation is considered to reflect bacillary replication dynamics and the host immune response. This analytic observational cross-sectional study was conducted retrospectively by reviewing secondary medical records and archived histopathology slides and paraffin blocks to assess the correlation and strength of association between tuberculous granulomatous histomorphology on Hematoxylin–Eosin staining and acid-fast bacilli (AFB) density on Modified Ziehl–Neelsen staining at the Unit Patologi Anatomik Rumah Sakit Pendidikan Prof. dr. Chairuddin Panusunan Lubis USU Medan and Rumah Sakit Columbia Asia Medan during 2023–2025, using consecutive sampling; 68 cases met the inclusion criteria. Histomorphology was categorized into epithelioid granuloma with or without Langhans-type giant cells with a necrotic mass, epithelioid granuloma with or without Langhans-type giant cells without necrosis, and acellular eosinophilic mass with inflammatory cells. AFB density was graded semi-quantitatively (0, +1, +2, +3) at 1000× magnification. Statistical analysis was performed using Fisher-Freeman-Halton exact test and Cramer's V. Most cases were extrapulmonary (95.59%), demonstrated epithelioid granuloma with necrosis (69.12%), and showed an AFB score of +1 (67.65%). Histomorphology showed a significant correlation with AFB density ($p<0.001$) with a strong association (Cramer's $V=0.59$), whereas correlations with organ group, age, and sex were not significant ($p>0.05$).

***Korespondensi**

Email:
delyuzar@usu.ac.id

DOI: http://doi.org/10.30743/ibnusina.v25i2.1152

INTRODUCTION

Based on the latest *Global Tuberculosis Report* (2023), tuberculosis (TB) remains a leading cause of death worldwide and the second deadliest infectious disease after Coronavirus Disease 2019 (COVID-19). This report estimates that 10.6 million people fell ill with TB globally, comprising 5.8 million men, 3.5 million women, and 1.3 million children, with approximately 1.3 million deaths attributed to the disease.[1]

Furthermore, Indonesia is identified as having the second-highest TB burden globally, accounting for 10% of all estimated incident cases. The largest shares of global TB cases are contributed by India (27%), followed by Indonesia (10%), China (7.1%), the Philippines (7.0%), Pakistan (5.7%), Nigeria (4.5%), Bangladesh (3.6%), and the Democratic Republic of the Congo (3.0%); these eight countries together account for approximately two-thirds of the total global cases.[1]

Pulmonary tuberculosis (PTB), or intrapulmonary tuberculosis, is the most common form, accounting for approximately 85% of global TB cases, whereas extrapulmonary tuberculosis (EPTB), defined as TB involving organs other than the lungs, accounts for about 15%. Reported EPTB sites include the lymph nodes, pleura, peritoneum and abdominal organs, skin, musculoskeletal system, central nervous system, pericardium, genitourinary system, and ocular structures.[2–5] EPTB may occur as primary infection at the initial site or as secondary disseminated disease, most commonly due to hematogenous or lymphatic spread from a primary organ, reactivation of latent TB, ingestion of infected sputum into the gastrointestinal tract, or local extension from adjacent organs.[5,6]

Intrapulmonary TB diagnosis uses complementary modalities, starting with chest radiological examination to detect suspicious pulmonary lesions, followed by sputum testing for acid-fast bacilli (AFB) to identify *Mycobacterium tuberculosis* (MTB) as an initial step in diagnosing active infection. Microbial culture on solid or liquid media serves as the gold standard because it enables definitive MTB identification. Histopathological examination via tissue biopsy or cytopathological evaluation using fine needle aspiration (FNA) of suspected TB lesions can also be performed to detect tuberculous granulomas. Molecular assays such as Polymerase Chain Reaction (PCR), Cartridge-Based Nucleic Acid Amplification Test (CBNAAT), and GeneXpert provide rapid detection of MTB deoxyribonucleic acid (DNA), whereas immunological tests such as Interferon Gamma Release Assays (IGRA) are used to distinguish active from latent infection by identifying the immune response.[5,7,8]

EPTB diagnosis is challenging because of its occult nature, difficulty in obtaining adequate samples, and paucibacillary characteristics. The International Standards for Tuberculosis Care recommend specimen collection from extrapulmonary infection sites, typically obtained by fine needle aspiration or biopsy for cytopathological, histopathological, and bacteriological examinations. Histopathological diagnosis is based on granulomatous inflammation characterized by aggregates of epithelioid histiocytes, a peripheral cuff of

lymphocytes and plasma cells, and epithelioid cells that may form Langhans giant cells with central necrosis within necrotizing granulomas.[9–11]

Tuberculosis lesions arise from continuous interactions between bacterial virulence and individual hypersensitivity and immunity to infection, and many authors have described a morphological spectrum reflecting disease stage and immune status. The presence of MTB in specimens is directly proportional to necrosis and inversely proportional to granuloma formation. Tuberculous lesions are morphologically categorized into: epithelioid granulomas with or without Langhans giant cells accompanied by necrotic masses, epithelioid granulomas with or without Langhans giant cells without necrotic masses, and acellular eosinophilic masses with inflammatory cells. Ziehl–Neelsen (ZN) staining is essential for identifying AFB in tissue sections, thereby supporting confirmation of tuberculosis.[12–16]

As a high-prevalence country, Indonesia continues to expand diagnostic examinations according to facility availability across healthcare levels; modality selection follows hospital resources and referral pathways, and histopathological examination remains an important confirmatory approach for suspected extrapulmonary tuberculosis when tissue biopsy is obtained. A thorough understanding of the histomorphological spectrum of tuberculous granulomatous inflammation is essential to strengthen diagnostic confidence among pathologists, particularly in immunocompromised patients (e.g., chronic comorbidities, HIV co-infection, or immunosuppressive drug use) in whom epithelioid granuloma formation may fail due to reduced CD4 cell levels.

However, despite the established role of histopathology in tuberculosis diagnosis, there is a paucity of quantitative data regarding the strength of association between specific histomorphological patterns and bacillary burden, particularly in high-burden populations with diverse extrapulmonary manifestations. Most existing literature focuses on qualitative descriptions without statistically measuring the magnitude of these correlations using effect size metrics like Cramer's V. Furthermore, the specific predictive value of the histomorphological spectrum for AFB density across both intrapulmonary and extrapulmonary sites requires further elucidation to improve diagnostic confidence in resource-limited settings. Therefore, this study aims to analyze the histomorphological spectrum of tuberculous granulomatous inflammation and quantify its correlation strength with AFB infiltration density, providing an empirical basis for interpreting biopsy samples with variable bacillary loads.

METHODS

This retrospective observational analytic study used a cross-sectional design by reviewing secondary medical record data and archived histopathological slides and paraffin blocks. It was conducted at the Unit Patologi Anatomik Rumah Sakit Pendidikan Prof. dr. Chairuddin Panusunan Lubis USU Medan and Rumah Sakit Columbia Asia Medan, using specimens collected during 2023–2025. This

design was selected to evaluate the correlation between the histomorphological spectrum of tuberculous granulomatous inflammation and AFB infiltration density without intervention or follow-up.

The study utilized a consecutive sampling method until the target population was captured. Case identification began by tracing slide and paraffin block numbers previously diagnosed with tuberculous granulomatous inflammation, followed by specimen adequacy verification. In instances where original slides were missing or damaged, paraffin blocks were recut to ensure representative sections for Hematoxylin and Eosin (H&E) and modified Ziehl-Neelsen (MZN) staining. The inclusion criteria comprised cases with complete medical records and adequate tissue specimens. Conversely, the exclusion criteria encompassed cases where the tissue within the paraffin block was exhausted or the blocks were missing or damaged. The minimum sample size was calculated using Cohen's w ($\alpha = 0.05$, 80% power, $w = 0.35$), yielding $n \approx 64$. During data collection, 68 eligible cases were obtained and all were included to improve precision of association estimates without changing the minimum requirement.

Clinical variables were extracted from medical records, while histopathological variables were obtained through the re-evaluation of H&E and MZN slides. To ensure diagnostic validity and minimize observer bias, microscopic interpretation was performed by two anatomical pathologists and one senior anatomical pathology resident. These reviewers were blinded to the clinical data, and any discordance in histomorphological classification or AFB grading was resolved through consensus. The histomorphological spectrum was classified into three categories: epithelioid granulomas with or without Langhans giant cells accompanied by necrotic masses; epithelioid granulomas with or without Langhans giant cells without necrotic masses; and acellular eosinophilic masses with inflammatory cells. AFB infiltration density was reported semi-quantitatively based on bacillary frequency: 0 (Negative), no AFB in the entire specimen; +1 (Focal), 1–99 AFB in 100 high-power fields (HPF); +2 (Disseminated), 1–10 AFB per HPF assessed in ≥ 50 HPF; and +3 (Numerous), > 10 AFB per HPF assessed in ≥ 20 HPF, all evaluated at 1000× oil immersion.

Data were analyzed using IBM SPSS software version 26.0. Categorical variables were summarized as frequencies and percentages. The Fisher-Freeman-Halton exact test was employed to analyze associations, as the assumption for expected cell counts (> 5) was violated in more than 20% of the contingency table cells. The strength of association was determined using the Cramer's V coefficient, interpreted as weak ($V < 0.30$), moderate (0.30–0.50), or strong ($V > 0.50$). Ethical approval was obtained from the Health Research Ethics Committee of the Faculty of Medicine, Universitas Sumatera Utara, and Rumah Sakit Pendidikan Prof. dr. Chairuddin Panusunan Lubis USU Medan (approval number 1393/KEPK/USU/2025).

RESULTS

The results of this study are summarized in Tables 1–8, providing a comprehensive overview of sample characteristics, frequency distributions, and descriptive–inferential correlation analyses across all variables. These findings are complemented by representative microscopic documentation, with Figure 1 illustrating the histomorphological spectrum of tuberculous granulomatous inflammation on H&E staining, and Figure 2 depicting the degrees of AFB infiltration density on MZN staining, both accompanied by complete figure captions.

Table 1. Characteristics of the study sample.

Variable	Frequency (n=68)	Percentage (100%)
Histomorphological spectrum of tuberculous granulomatous inflammation		
Epithelioid granulomas with or without Langhans giant cells accompanied by necrotic masses	47	69.12%
Epithelioid granulomas with or without Langhans giant cells without necrotic masses	17	25.00%
Acellular eosinophilic masses with inflammatory cells	4	5.88%
Acid-Fast Bacilli infiltration density		
0 (negative)	3	4.41%
+1 (focal)	46	67.65%
+2 (disseminated)	15	22.06%
+3 (numerous)	4	5.88%
Tuberculosis infection location by organ group		
Intrapulmonary	3	4.41%
Extrapulmonary	65	95.59%
Tuberculosis infection location by specific organ		
Larynx	1	1.47%
Lung parenchyma, tracheobronchial	3	4.41%
Pleura	7	10.30%
Mediastinum	1	1.47%
Lymph nodes	35	51.48%
Skin, subcutaneous tissue	6	8.82%
Breast	2	2.94%
Musculoskeletal	1	1.47%
Ileum, colon, appendix, omentum, peritoneum	6	8.82%
Uterus, adnexa	3	4.41%
Prostate	1	1.47%
Anorectal	2	2.94%
Age group		
0–14 years	2	2.94%
15–24 years	24	35.29%
25–44 years	22	32.35%
45–64 years	9	13.24%
≥65 years	11	16.18%
Sex		
Male	19	27.94%
Female	49	72.06%

Table 2. Frequency distribution and correlation analysis between the histomorphological spectrum of tuberculous granulomatous inflammation and Acid-Fast Bacilli infiltration density.

Histomorphological spectrum of tuberculous granulomatous inflammation (H&E)	AFB infiltration density (MZN)				p-value	Cramer's V
	0	+1	+2	+3		
	n=3 (4.41%)	n=46 (67.65%)	n=15 (22.06%)	n=4 (5.88%)		
Epithelioid granulomas with or without Langhans giant cells accompanied by necrotic masses	1 (1.47%)	31 (45.59%)	14 (20.59%)	1 (1.47%)	< 0.001	0.59
Epithelioid granulomas with or without Langhans giant cells without necrotic masses	1 (1.47%)	15 (22.06%)	1 (1.47%)	0 (0.00%)		
Acellular eosinophilic masses with inflammatory cells	1 (1.47%)	0 (0.00%)	0 (0.00%)	3 (4.41%)		

*Fisher-Freeman-Halton Exact Test.

Table 3. Frequency distribution and correlation analysis between the histomorphological spectrum of tuberculous granulomatous inflammation and infection location by organ group.

Histomorphological spectrum of tuberculous granulomatous inflammation (H&E)	Infected organ group location		p-value	Cramer's V
	Intrapulmonary	Extrapulmonary		
	n=3 (4.41%)	n=65 (95.59%)		
Epithelioid granulomas with or without Langhans giant cells accompanied by necrotic masses	1 (1.47%)	46 (67.65%)	0.306	0.21
Epithelioid granulomas with or without Langhans giant cells without necrotic masses	2 (2.94%)	15 (22.06%)		
Acellular eosinophilic masses with inflammatory cells	0 (0.00%)	4 (5.88%)		

*Fisher-Freeman-Halton Exact Test.

Table 4. Frequency distribution and correlation analysis between the histomorphological spectrum of tuberculous granulomatous inflammation and age groups.

Histomorphological spectrum of tuberculous granulomatous inflammation (H&E)	Age group in years					p-value	Cramer's V
	0–14	15–24	25–44	45–64	≥65		
	n=2 (2.94%)	n=24 (35.29%)	n=22 (32.35%)	n=9 (13.24%)	n=11 (16.18%)		
Epithelioid granulomas with or without Langhans giant cells accompanied by necrotic masses	2 (2.94%)	20 (29.41%)	16 (23.53%)	5 (7.36%)	4 (5.88%)	0.170	0.30
Epithelioid granulomas with or without Langhans giant cells without necrotic masses	0 (0.00%)	3 (4.41%)	5 (7.35%)	4 (5.88%)	5 (7.36%)		
Acellular eosinophilic masses with inflammatory cells	0 (0.00%)	1 (1.47%)	1 (1.47%)	0 (0.00%)	2 (2.94%)		

*Fisher-Freeman-Halton Exact Test.

Table 5. Frequency distribution and correlation analysis between the histomorphological spectrum of tuberculous granulomatous inflammation and sex.

Histomorphological spectrum of tuberculous granulomatous inflammation (H&E)	Sex		p-value	Cramer's V
	Male	Female		
	n=19 (27.94%)	n=49 (72.06%)		
Epithelioid granulomas with or without Langhans giant cells accompanied by necrotic masses	15 (22.06%)	32 (47.06%)	0.307	0.18
Epithelioid granulomas with or without Langhans giant cells without necrotic masses	4 (5.88%)	13 (19.12%)		
Acellular eosinophilic masses with inflammatory cells	0 (0.00%)	4 (5.88%)		

*Fisher-Freeman-Halton Exact Test.

Table 6. Frequency distribution and correlation analysis between Acid-Fast Bacilli infiltration density and infection location by organ group.

AFB infiltration density (MZN)	Infected organ group location		p-value	Cramer's V
	Intrapulmonary	Extrapulmonary		
	n=3 (4.41%)	n=65 (95.59%)		
0 (negative)	1 (1.47%)	2 (2.94%)	0.154	0.32
+1 (focal)	2 (2.94%)	44 (64.71%)		
+2 (disseminated)	0 (0.00%)	15 (22.06%)		
+3 (numerous)	0 (0.00%)	4 (5.88%)		

*Fisher-Freeman-Halton Exact Test.

Table 7. Frequency distribution and correlation analysis between Acid-Fast Bacilli infiltration density and age groups.

AFB infiltration density (MZN)	Age group in years					p-value	Cramer's V
	0–14	15–24	25–44	45–64	≥65		
	n=2 (2.94%)	n=24 (35.29%)	n=22 (32.35%)	n=9 (13.24%)	n=11 (16.18%)		
0 (negative)	0 (0.00%)	2 (2.94%)	0 (0.00%)	0 (0.00%)	1 (1.47%)	0.730	0.20
+1 (focal)	1 (1.47%)	15 (22.06%)	15 (22.06%)	6 (8.82%)	9 (13.24%)		
+2 (disseminated)	1 (1.47%)	6 (8.82%)	5 (7.35%)	3 (4.42%)	0 (0.00%)		
+3 (numerous)	0 (0.00%)	1 (1.47%)	2 (2.94%)	0 (0.00%)	1 (1.47%)		

*Fisher-Freeman-Halton Exact Test.

Table 8. Frequency distribution and correlation analysis between Acid-Fast Bacilli infiltration density and sex.

AFB infiltration density (MZN)	Sex		p-value	Cramer's V
	Male	Female		
	n=19 (27.94%)	n=49 (72.06%)		
0 (negative)	2 (2.94%)	1 (1.47%)	0.187	0.25
+1 (focal)	14 (20.59%)	32 (47.06%)		
+2 (disseminated)	3 (4.41%)	12 (17.65%)		
+3 (numerous)	0 (0.00%)	4 (5.88%)		

*Fisher-Freeman-Halton Exact Test.

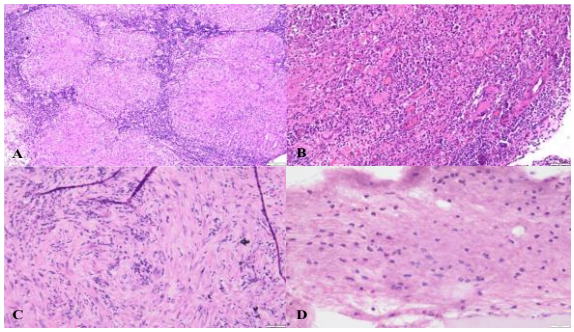

Figure 1. Biopsy tissue specimens from various organs stained with H&E. A. Cervical lymph node showing central necrosis with well-differentiated epithelioid granulomas and Langhans giant cells (100×). **B.** Breast showing abscess formation, characterized by a necrotic mass massively infiltrated by polymorphonuclear (PMN) and mononuclear (MN) inflammatory cells, with identifiable epithelioid cells and Langhans giant cells (200×). **C.** Pleura showing epithelioid granulomas without necrotic areas, with Langhans giant cells in one focus (200×). **D.** Mediastinum dominated by extensive necrotic masses infiltrated by PMN and MN inflammatory cells (400×).

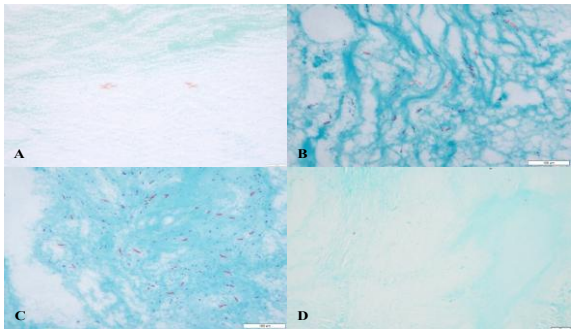

Figure 2. Expression of MZN staining for AFB in biopsy tissue specimens from various organs. **A.** Bronchus showing eosinophilic rod-shaped AFB; overall evaluation consistent with +1 (focal), defined as 1–99 AFB in 100 high-power fields (1000×). **B.** Ileum showing eosinophilic rod-shaped AFB; overall evaluation consistent with +2 (disseminated), defined as 1–10 AFB per high-power field assessed in ≥50 high-power fields (1000×). **C.** Thoracic vertebra showing eosinophilic rod-shaped AFB; overall evaluation consistent with +3 (numerous), defined as >10 AFB per high-power field assessed in ≥20 high-power fields (1000×). **D.** Lymph node showing no AFB in the entire specimen, interpreted as 0 (negative) (1000×).

DISCUSSION

This study analyzed 68 cases of tuberculous granulomatous inflammation. The sample included 3 intrapulmonary cases (4.41%) and 65 extrapulmonary cases (95.59%). This distribution contrasts with Baykan (2022), where intrapulmonary tuberculosis predominated (70–80%) and extrapulmonary cases accounted for ~15–20%.[4] This discrepancy is expected because pulmonary tuberculosis is primarily diagnosed using symptoms, radiologic findings, and sputum AFB testing. Consequently, there is a lower clinical requirement for tissue biopsy in pulmonary cases. Pattamapaspong (2024) reported that active tuberculosis may present as solitary pulmonary nodules mimicking neoplasia.[17] Consistently, all intrapulmonary cases in this study were nodular lesions initially suspected as neoplastic and later confirmed as tuberculous granulomas. The predominance of lymph nodes among extrapulmonary sites aligns with Rukmi (2025), identifying lymph nodes as the most common extrapulmonary manifestation.[18] Such broad involvement reflects the capacity of MTB to infect diverse organs.[4,18,19]

The age distribution comprised five groups, with the highest proportions in the 15–24 years (35.29%) and 25–44 years (32.35%) groups. This pattern is consistent with reports indicating that tuberculosis predominantly affects productive-age populations in high-burden settings.[1] A cohort study in Bangladesh (2022) reported peak incidence in the third and fourth decades, attributed to environmental and socioeconomic factors.[20] Older age remains a risk group due to comorbidities and immune decline, whereas pediatric cases are less represented in biopsy series.[21] These variations likely reflect referral-hospital characteristics and institutional case mix.[22]

Sex distribution showed female predominance (49 cases; 72.06%). In contrast, the *Global Tuberculosis Report* (2023) reported higher pulmonary tuberculosis prevalence among males.[1] Horton (2016) attributed higher male risk to behavioral factors and environmental exposures.[23] Because biopsy-based studies may differ from population-prevalence data, the female predominance here likely reflects the demographic characteristics of cases referred to anatomical pathology services.[22]

The histomorphologic spectrum was dominated by epithelioid granulomas with or without Langhans giant cells accompanied by necrotic masses (69.12%). This was followed by epithelioid granulomas with or without Langhans giant cells without necrotic masses (25.00%) and acellular eosinophilic masses with inflammatory cells (5.88%). This distribution is consistent with classic tuberculous granulomas during active infection. Epithelioid granulomas with or without Langhans giant cells without necrotic masses may occur in earlier disease stages or when cellular immunity preserves granuloma organization. Conversely, acellular eosinophilic masses represent a rarer pattern associated with granuloma structural breakdown or high bacillary burden. Together, these patterns represent the practical diagnostic spectrum of tuberculosis.[24,25]

AFB density was predominantly scored as +1 (67.65%), reflecting the typically

paucibacillary nature of tuberculosis in tissue. This pattern aligns with Chakravorty (2017) and Purohit (2015), who highlighted the limited sensitivity of ZN staining.[11,26] Score +1 indicates uneven bacillary distribution, whereas scores +2 and +3 reflect higher bacillary loads, particularly in necrotic lesions. Score +3 supports the concept that necrotic tissue harbors higher bacillary concentrations. AFB score 0 remains compatible with TB because bacilli may be focal and missed in the examined plane.[9,26] Negative AFB staining does not exclude tuberculosis when morphology is supportive.

Frequency analysis showed that epithelioid granulomas with or without Langhans giant cells accompanied by necrotic masses were most common (47 cases; 69.12%). In this group, AFB scores were +1 in 31 cases and +2 in 14 cases. Epithelioid granulomas with or without Langhans giant cells without necrotic masses accounted for 17 cases (25.00%), predominantly with AFB score +1. Acellular eosinophilic masses with inflammatory cells were identified in 4 cases (5.88%), including three with AFB score +3. Correlation analysis demonstrated a significant association between histomorphologic spectrum and AFB density ($p < 0.001$), with a strong strength of association (Cramer's $V = 0.59$).[11,24–26]

Epithelioid granulomas with or without Langhans giant cells accompanied by necrotic masses were associated with AFB scores +1 and +2. Delyuzar and Dedy (2019) reported that organized granulomas often show typical morphology despite scant AFB staining.[27] Humairah and Delyuzar (2020) demonstrated dominant IFN-γ expression in organized granulomas, reflecting a strong Th1 response that limits bacillary replication.[28] These findings support the predominance of low-to-moderate AFB scores in this granuloma type.

Epithelioid granulomas with or without Langhans giant cells without necrotic masses were also dominated by AFB score +1 (22.06%). This is consistent with a stable granulomatous phase where immune responses restrict bacillary spread. Delyuzar and Nadjib (2017) reported that compact lesions often contain very few bacilli yet correlate strongly with PCR-confirmed MTB.[29] Other studies report that non-necrotizing granulomas are almost invariably paucibacillary.[30] The present findings are concordant, as most cases showed very low bacillary counts.

Acellular eosinophilic masses with inflammatory cells showed a distinct pattern, with three of four cases exhibiting AFB score +3 (4.41%). Extensive necrosis without organized granulomas reflects severe tissue destruction, facilitating bacillary accumulation. Humairah and Nadjib (2021) demonstrated that increased IL-4 expression in destructive lesions is associated with higher bacillary loads.[30] Experimental studies show that caseous necrosis centers contain the highest bacillary concentrations.[25] These findings indicate that the histomorphologic spectrum mirrors bacillary replication dynamics and disease activity within tissue.

Clinically, these results underscore the diagnostic utility of histomorphological profiling for therapeutic decisions. The strong association observed (Cramer's $V = 0.59$) confirms that the entire spectrum reflects

integral stages of tuberculosis with distinct bacillary burdens. While necrotic masses often correlate with active replication, this study validates that granulomas without necrotic masses are also diagnostically significant. Pathologists should maintain high confidence in diagnosing tuberculosis based on morphological evidence, even with negative or focal AFB staining. This approach prevents diagnostic oversight and justifies timely treatment initiation.

Across organ groups, epithelioid granulomas with or without Langhans giant cells accompanied by necrotic masses remained predominant (69.12%). No significant association was observed between histomorphologic spectrum and organ group ($p = 0.306$, Cramer's $V = 0.21$). This uniformity reflects the fact that granuloma formation is governed by immune mechanisms that operate similarly across tissues.[22] Asian studies likewise report necrotizing epithelioid granulomas as the dominant pattern across various extrapulmonary sites.[18,20] Thus, anatomic location influences disease distribution rather than granuloma morphology.

Regarding age, no significant association was observed with the histomorphologic spectrum ($p = 0.170$, Cramer's $V = 0.30$). These findings align with Diedrich (2016), reporting that both necrotizing and non-necrotizing granulomas occur across ages when T-cell immunity is maintained.[21] Thus, granuloma morphology reflects host immune dynamics rather than age. Similarly, no statistically significant association was found between histomorphologic spectrum and sex ($p = 0.307$, Cramer's $V = 0.18$). Granuloma morphology remains comparable between sexes because it is driven by macrophage activation and immune responses.[21,23]

AFB score +1 was the most frequent category across all organ groups (67.65%). No significant association was found between AFB density and organ group ($p = 0.154$, Cramer's $V = 0.32$). This supports Baykan (2022), who noted that tissue AFB detection depends on organism load rather than location.[4] Similarly, AFB density did not correlate significantly with age ($p = 0.730$) or sex ($p = 0.187$). Kumar (2021) emphasized that paucibacillary granulomas occur across demographics when cellular immunity limits replication.[31] Accordingly, tissue AFB density reflects immune-response variability and lesion characteristics rather than age or sex.[21,23]

LIMITATIONS OF THE STUDY

This study has several limitations inherent to its retrospective design and hospital-based setting. First, the use of consecutive sampling in tertiary referral centers introduces selection bias, explaining the marked predominance of extrapulmonary cases (95.59%). PTB is typically diagnosed via sputum analysis and radiology without tissue biopsy; thus, our dataset represents the spectrum of cases requiring histopathological confirmation rather than the prevalence in the general population. Consequently, the small sample size of intrapulmonary cases ($n = 3$) limits the generalizability of findings specific to lung pathology. Second, the diagnosis relied on histomorphology and MZN staining without confirmation by Nucleic Acid Amplification

Tests. While this reflects routine practice in resource-limited settings, it precludes the definitive exclusion of non-tuberculous mycobacteria in AFB-negative cases. Finally, histopathological evaluation was limited to single tissue sections, which may underestimate AFB density due to the focal nature of MTB distribution.

CONCLUSION AND FUTURE DIRECTIONS

This study demonstrates a significant correlation with a strong strength of association between the histomorphological spectrum of tuberculous granulomatous inflammation and AFB infiltration density. Specifically, acellular eosinophilic masses are directly proportional to bacillary load and inversely proportional to granuloma formation, whereas organized epithelioid granulomas typically exhibit paucibacillary characteristics. This association reflects the host immune capacity for bacillary containment; where an effective response limits bacterial replication within organized structures, while structural breakdown facilitates bacillary accumulation. Clinically, these findings underscore the importance of histomorphological profiling as a robust diagnostic tool, justifying the initiation of TB treatment even in AFB-negative cases when characteristic granulomatous patterns are present. Given that correlations with PCR and cytokine profiles (IFN-γ and IL-4) have been previously reported, future research is suggested to employ Polyclonal MTB or Anti-MPT64 Immunohistochemistry for more sensitive antigen detection, and to evaluate macrophage polarization (M1 vs M2) to validate whether M2 phenotype (CD163) dominance correlates with high bacillary loads in necrotic lesions, distinct from M1 (CD68, iNOS) phenotypes in solid epithelioid granulomas.

ACKNOWLEDGMENTS

The authors wish to thank the Department of Anatomical Pathology, Faculty of Medicine, Universitas Sumatera Utara for their encouragement and support in this project.

REFERENCES

1. World Health Organization. Global tuberculosis report 2023. Geneva: World Health Organization. https://www.who.int/teams/global-tuberculosis-programme/tb-reports/global-tuberculosis-report-2023. Published 2023. Accessed January 24, 2025.
2. Bhuyan G, Deshpande M. Patterns of tubercular lymphadenitis encountered in routine cytology reporting: An experience in a tertiary care center of Northeastern part of India. *MRIMS J Heal Sci*. 2024;12(1):67-70. doi:10.4103/mjhs.mjhs_59_23
3. Arega B, Mersha A, Minda A, et al. Epidemiology and the diagnostic challenge of extra-pulmonary tuberculosis in a teaching hospital in Ethiopia. *PLoS One*. 2020;15(12):e0243945. doi:10.1371/journal.pone.0243945
4. Baykan AH, Sayiner HS, Aydin E, Koc M, Inan I, Erturk SM. Extrapulmonary Tuberculosis: An Old but Resurgent Problem. *Insights Imaging*. 2022;13(1):39. doi:10.1186/s13244-022-01172-0
5. Gopalaswamy R, Dusthackeer VNA, Kannayan S, Subbian S. Extrapulmonary tuberculosis—an update on the diagnosis, treatment and drug resistance. *J Respir*.

2021;1(2):141-164. doi:10.3390/jor1020015

6. Sharma SK, Mohan A, Kohli M. Extrapulmonary tuberculosis. *Expert Rev Respir Med*. 2021;15(7):931-948. doi:10.1080/17476348.2021.1927718
7. Gautam H, Agrawal SK, Verma SK, Singh UB. Cervical tuberculous lymphadenitis: Clinical profile and diagnostic modalities. *Int J Mycobacteriology*. 2018;7(3):212-216. doi:10.4103/ijmy.ijmy_99_18
8. Gain D, Nikhil P V. Cytomorphological Patterns of AFB Positive Tubercular Lymphadenitis: A Cross-sectional Study. *Natl J Lab Med*. 2024;13(01):56-59. doi:10.7860/NJLM/2024/63914.2822
9. Purohit M, Mustafa T. Laboratory diagnosis of extra-pulmonary tuberculosis (EPTB) in resource-constrained setting: state of the art, challenges and the need. *J Clin diagnostic Res JCDR*. 2015;9(4):EE01. doi:10.7860/JCDR/2015/.5792
10. Shah KK, Pritt BS, Alexander MP. Histopathologic Review of Granulomatous Inflammation. *J Clin Tuberc Other Mycobact Dis*. 2017;7:1-12. doi:10.1016/j.jctube.2017.02.001
11. Tahseen S, Ambreen A, Ishtiaq S, et al. *The Value of Histological Examination in the Diagnosis of Tuberculous Lymphadenitis in the Era of Rapid Molecular Diagnosis*. Vol 12. Nature Publishing Group UK London; 2022. doi:10.1038/s41598-022-12660-0
12. Dharmalingam S, Sutrakar SK, Jatav J, Verma S. A cytological study on peripheral lymphadenopathy in a tertiary care center with special reference to tuberculous lymphadenitis. *Asian J Med Sci*. 2022;13(9):227-231. doi:10.3126/ajms.v13i9.45077
13. Vimal S, Dharwadkar A, Chandanwale Shrish S, Verma V, Khandelwal A. Fine needle aspiration cytology in the diagnosis of Tuberculous lymphadenitis and utility of Ziehl Neelsen stain benefits and pitfalls. *Int J Med Res Rev*. 2016;4(8):1466-1475. doi:10.17511/ijmrr.2016.i08.30
14. Pradhan A, Poudyal P, Upadhyaya P, Pokhrel S. Cytomorphological spectrums in tuberculous lymphadenitis: understanding the stages of disease. *J BP Koirala Inst Heal Sci*. 2018;1(2):21-29. doi:10.3126/jbpkihs.v1i2.22074
15. Handa U, Mundi I, Mohan S. Nodal tuberculosis revisited: a review. *J Infect Dev Ctries*. 2012;6(01):6-12. doi:10.3855/jidc.2090
16. Ahmed S, Ansari HA, Fatima N. A clinicopathological study of fine needle aspirates of lymph nodes from patients with suspected tubercular lymphadenopathy: analysis of 640 cases from a tertiary health care centre in North India. *Int J Heal Sci Res*. 2022;12:201-208. doi:10.52403/ijhsr.20220127
17. Pattamapaspong N, Kanthawang T, Peh WCG, Hammami N, Bouaziz MC, Ladeb MF. Imaging of thoracic tuberculosis: pulmonary and extrapulmonary. *BJR| Open*. 2024;6(1):tzae031. doi:10.1093/bjro/tzae031
18. Rukmi KW, Sasongko A, Suyuthie HD, et al. Clinical and Histopathological Findings of Extrapulmonary Tuberculosis in Multiple Organ Sites. *J Kedokt dan Kesehat Mhs MalikusSaleh*. 2025;4(3):98-116. https://ojs.unimal.ac.id/galenical/article/view/21895/9480.
19. Liu Q, Xu F, Liu Q, Liu X. Comparative analysis of five etiological detecting techniques for the positive rates in the diagnosis of tuberculous granuloma. *J Clin Tuberc Other Mycobact Dis*. 2023;32:100378.

doi:10.1016/j.jctube.2023.100378

20. Azad KAK, Chowdhury T. Extrapulmonary Tuberculosis (Eptb): An Overview. *Bangladesh J Med*. 2022;33(2):130-137. doi:10.3329/bjm.v33i2.59285

21. Diedrich CR, O'hern J, Wilkinson RJ. HIV-1 and the Mycobacterium tuberculosis granuloma: A systematic review and meta-analysis. *Tuberculosis*. 2016;98:62-76. doi:10.1016/j.tube.2016.02.010

22. Sharma SK, Ryan H, Khaparde S, et al. Index-TB guidelines: guidelines on extrapulmonary tuberculosis for India. *Indian J Med Res*. 2017;145(4):448-463. doi:10.4103/ijmr.IJMR_1950_16

23. Horton KC, MacPherson P, Houben RMGJ, White RG, Corbett EL. Sex differences in tuberculosis burden and notifications in low-and middle-income countries: a systematic review and meta-analysis. *PLoS Med*. 2016;13(9):e1002119. doi:10.1371/journal.pmed.1002119

24. Dheda K, Barry CE, Maartens G. Tuberculosis. *Lancet*. 2016;387(10024):1211-1226. doi:10.1016/S0140-6736(15)00151-8

25. Ulrichs T, Kaufmann SHE. New insights into the function of granulomas in human tuberculosis. *J Pathol A J Pathol Soc Gt Britain Irel*. 2006;208(2):261-269. doi:10.1002/path.1906

26. Chakravorty S, Simmons AM, Rowneki M, et al. The new Xpert MTB/RIF Ultra: improving detection of Mycobacterium tuberculosis and resistance to rifampin in an assay suitable for point-of-care testing. *MBio*. 2017;8(4):10-1128. doi:10.1128/mbio.00812-17

27. Delyuzar D, Sinulingga AB, Suryadi D. Association between fine-needle aspiration cytological features and CD4 level in human immunodeficiency virus-associated tuberculous lymphadenitis patients admitted to Haji Adam Malik hospital in 2017. *Open Access Maced J Med Sci*. 2019;7(20):3475. doi:10.3889/oamjms.2019.449

28. Lubis HM, Ganie RA, Delyuzar, Eyanoer PC, Munir D. Immunocytochemical Expression of IFN-γ and IL-4 in Tuberculous Lymphadenitis with Dark Oval Bodies. *Open Access Maced J Med Sci*. 2020;8:806-809. doi:10.3889/oamjms.2020.4085

29. Delyuzar D, Lubis MN, Amir Z, Kusumawati L. Tuberculosis with eosinophilic mass and dark brown particles. Jurnal Respirologi Indonesia. https://arsip.jurnalrespirologi.org/wp-content/uploads/2018/04/JRI-Jul-2017-37-195.pdf. Published 2017. Accessed January 24, 2025.

30. Lubis HML, Lubis MND, Delyuzar D. Interleukin-4 cytokine as an indicator of the severity of tuberculous lymphadenitis. *Open Access Maced J Med Sci*. 2021;9(A):82-86. doi:10.3889/oamjms.2021.5667

31. Kumar R, Subbian S. Immune correlates of non-necrotic and necrotic granulomas in pulmonary tuberculosis: A pilot study. *J Respir*. 2021;1(4):248-259. doi:10.3390/jor1040023